Refined scaling hypothesis for anomalously diffusing processes

R. Badii[*,1], P. Talkner

General Energy Research Department, Paul Scherrer Institute, 5232 Villigen, Switzerland

Abstract

Anomalous diffusion in artificial and natural stochastic processes is studied through the statistics of small-scale fluctuations. It is shown that the moments of certain locally averaged quantities, such as the square or absolute increments, do not scale like power laws, as generally assumed. A much improved scaling function is deduced, in analogy with a procedure first applied to nearest-neighbour dimension estimators. Extremely accurate determination of the scaling exponents is thus possible. Our refined formula is immediately applicable to the analysis of time series in turbulence, physiology, or economics.

Keywords: Scaling; Anomalous diffusion; Stochastic self-affinity; Fractional Brownian motion; Turbulence; EEG; Economics

1. Introduction

Anomalous diffusion [1,2] is a widespread phenomenon occurring in quite disparate fields, such as fluid turbulence, solid-state and plasma physics, nonlinear dynamics, chemistry, physiology, and economics. Its usual characterization is obtained by considering a random walker at the position $x_{t_0} \in \mathbb{R}^D$ at time t_0, and the second moment $S_2(t; t_0) = \langle d_{t_0}^2(t) \rangle$ of the walker's displacement $d_{t_0}(t) = x_{t_0+t} - x_{t_0}$ in a time t, where $\langle \cdot \rangle$ denotes an ensemble average (for a path with stationary increments, the averages are independent of t_0). If $S_2(t; t_0)$ does not scale linearly with t for $t \to \infty$, as in the case of Brownian motion, the walker is said to undergo anomalous diffusion (AD).

This behaviour is usually accompanied by long-ranged correlations (with power spectra of the $\omega^{-\alpha}$ type) and is associated with fractal or self-affine [3,4] features of the measured signals.[2]

A quantitative description of the process is often provided in the form of scaling exponents ζ_p estimated from the moments of the increments $d_{t_0}(t)$. Restricting the analysis to scalar time series and assuming the stationarity of the increments $d_{t_0}(t) = x_{t_0+t} - x_{t_0}$, ζ_p is then defined as

$$\langle d^p(t) \rangle \sim t^{\zeta_p} , \tag{1}$$

where the symbol $\sim$ denotes the behaviour of the expectation for t in some interval $[t_{\min}, t_{\max}]$. For stochastic processes X_t satisfying the self-affinity equality in distribution

$$(X_{\gamma t}) \overset{D}{=} (\gamma^H X_t) . \tag{2}$$

Eq. (1) holds for all t with $\zeta_p = pH$, where H is the Hurst index [3] (Brownian motion corresponding to the case $H = \frac{1}{2}$) and $\gamma > 0$ a rescaling factor. If $d(t)$ is a (longitudinal) velocity difference measured in a turbulent fluid, the scaling law Eq. (1) is approximately verified in the so-called inertial range $[t_{\min}, t_{\max}]$ and ζ_p grows sublinearly with p [5].

In the attempt to explain this behaviour, a *refined hypothesis* was proposed in Ref. [6,7], by taking into account the moments

$$\langle \varepsilon^p(t) \rangle \sim t^{\tau_p} \tag{3}$$

of the energy dissipation rate $\varepsilon(t)$ averaged over an interval of length t. This quantity can be simply expressed in terms of the process increments $d(t)$, as we shall illustrate in the following section. The fluctuations of the velocity and the dissipation field were then linked by assuming

$$\langle d^{3p}(t) \rangle \sim t^p \langle \varepsilon^p(t) \rangle , \tag{4}$$

which yields the following relation between the scaling exponents:

$$\zeta_{3p} = p + \tau_p . \tag{5}$$

The motivation for this conjecture is founded in the well-known formula [8]

$$\langle d^3(t) \rangle \sim -\frac{4}{5} t \langle \varepsilon(t) \rangle , \tag{6}$$

which was deduced from the Navier–Stokes (NS) equations. Indeed, these satisfy a similarity property involving a Hurst index $H = \frac{1}{3}$ [5], which explains the third power of d in Eq. (6). The same approach, with slightly different definitions of $\varepsilon(t)$, is commonly adopted in other fields, such as those mentioned in the opening.

In the present paper, we show that relation (3) is neither verified, nor motivated, and replace it by a different, refined scaling law. Analysis of artificial signals obeying (2) clearly illustrates the precision that can be achieved with the improved formula. Results

---

[2] Generally, spatio-temporal patterns are measured. In the following, however, we concentrate on time-series, for simplicity.

obtained on turbulent and physiological time series are also presented. Discussion of turbulent fluctuations is, however, deferred to a subsequent publication, because of the physical implications of the new approach [9].

2. Failure of "commonplace" power-law scaling

Consider a stochastic process $X = \{X(t)\}$ ($t \in \mathbb{R}$), sampled at times $t_i = i\Delta t$, and define its k-step increments as

$$d_i(k) = x_{i+k} - x_i \, , \tag{7}$$

where $x_i = X(t_i)$. The roughness of the sample path can be estimated from the variation of X over intervals $I_i(t) = [t_i, t_i + t]$ of length t. For convenience, we shall express all scaling laws in terms of the number

$$\ell = \frac{t}{\Delta t} \tag{8}$$

of sampling steps in the interval. The usage of the letter ℓ conforms to the common symbology of turbulence studies, where this quantity is indifferently either a spatial or a temporal length. In particular, we compute the total k-step square variation

$$E_i(\ell; k) = \sum_{j=i}^{i+\ell-1} d_j^2(k) \tag{9}$$

over $I_i(t)$ and obtain the locally averaged analogue of the energy dissipation rate $\varepsilon_i(\ell)$ in turbulence by the following division:

$$\varepsilon_i(\ell; k) = E_i(\ell; k)/\ell \, . \tag{10}$$

This is the quantity that appears in Eqs. (3), (4), and (6). Since it is rather easy to compute from a time series, the sum (9) is commonly used also in turbulence, although the actual-energy dissipation rate is properly defined in terms of the strain tensor [5].[3] Notice that expression (9) reduces to the actual order-2 variation for $k = 1$.

Let now X be a zero-mean Gaussian process satisfying relation (2) for any $\gamma \geqslant 0$ and, consequently, having the covariance function

$$\text{cov}\{x(t), x(t')\} = \tfrac{1}{2}[|t|^{2H} + |t'|^{2H} - |t - t'|^{2H}] \, , \tag{11}$$

where $H \in (0, 1)$ is the Hurst index. As it is well known, fractional Brownian motion (fBm) [10] belongs to this class of models. Its increments are stationary (they satisfy Eq. (1)) and correlated (except at $H = \tfrac{1}{2}$, i.e., for ordinary Brownian motion). Although not a faithful representation of real stochastic processes, such as those encountered in turbulence, physiology or economics, these models constitute a useful ground for testing theories under controlled conditions and with high numerical precision.

---

[3] For this reason, the quantity $\varepsilon_i(\ell; k)$ in Eq. (10) is known as a one-dimensional "surrogate" for the full three-dimensional expression, which is hardly available from experiments. Although these two quantities are conjectured to scale in the same way with ℓ, their statistical properties are definitely different.

When $\ell \to \infty$, with finite t, the dependence of ε on k can be expressed as

$$\varepsilon_i(\ell; k) \sim k^{2H} , \tag{12}$$

irrespectively of i. Therefore, the scaling of $E_i(\ell; k)$ (possibly averaged over all i) with k provides an estimate of H, whereas its dependence on ℓ is not especially relevant in the study of stochastic processes. The smaller H, the rougher the path: the latter's dimension D, in fact, is given by $D = 2 - H$.

More generally, k is the yard-stick for the evaluation of the increments $d_i(k)$. In the case of turbulence, these are the gradients of the velocity field (up to a division by k). Hence, k must be chosen in a narrow interval, depending on the sampling time Δt. If k is too small, instrumental (or numerical) noise prevails; if it is too large, $d(k)/k$ fails to approximate a gradient. Usually, moments of $E_i(\ell; k)$ in turbulence are studied as functions of ℓ and the k-dependence is ignored. As shown in Ref. [11], this is a substantial source of errors.

Even worse is the disagreement between Eq. (3) and reality. Plots of $\langle \varepsilon^2(\ell; k) \rangle$ vs. ℓ, for fixed k, such as those displayed in Fig. 1 for various fBms, are all but linear in a doubly-logarithmic scale. Evidently, Eq. (3) is wrong. The deviations from linearity get more pronounced for larger $|p|$.

In the next section, we propose a complete scaling law, which accounts for both dependences, on k and on ℓ, of the ε-moments.

3. The refined scaling law

A typical graph of $E_i(\ell; k)$ versus ℓ ($k = 5$) is drawn in Fig. 2 for a fBm with $H = 0.33$ (simulated as explained in Ref. [12]). The curve is strongly reminiscent of a Devil's staircase. Our aim is to evaluate the probability $\rho_\ell(E)\Delta E$ for $E(\ell; k)$ to lie in the interval $[E, E + \Delta E]$, since its moments yield τ_p, according to Eqs. (3) and (10). This task can be accomplished in a straightforward, exact way for ordinary Brownian motion. For stochastic processes with correlated increments and non-Gaussian statistics, however, a few approximations are necessary: notwithstanding this, the result will be surprisingly accurate even for processes which do not satisfy the conditions we impose.

Let us first assume $X_H = X_{1/2}$ to be the Wiener process (Brownian motion without drift) and $\{x_1, x_2, \ldots, x_n\}$ a time series obtained from it by sampling with a step Δt. We also take increments $d_i(k)$ over one step (i.e., $k = 1$), so that $E(\ell; k)$, Eq. (9), is the sum of ℓ uncorrelated terms. Then, the density $\rho_\ell(E)$ is just the chi-square (χ^2) density with ℓ degrees of freedom, in which E represents the χ^2 function [13]:

$$\rho_\ell(E) = \frac{E^{\ell/2 - 1}}{(\sigma\sqrt{2})^\ell \, \Gamma(\ell/2)} e^{-E/2\sigma^2} , \tag{13}$$

where σ is the variance of the increments d_i and Γ the gamma function. Hence, the moments read

$$\langle E^p(\ell) \rangle = \int_0^\infty E^p \rho_\ell(E) \, dE \sim \frac{\Gamma(\ell/2 + p)}{\Gamma(\ell/2)} , \tag{14}$$

up to the here irrelevant prefactor $(2\sigma^2)^p$. In the limit $\ell \to \infty$, the ratio on the r.h.s. goes like ℓ^p. Comparison of this behaviour with the scaling law $\langle E^p \rangle \sim \ell^{p+\tau_p}$, resulting from Eqs. (3) and (10), leads to $\tau_p = 0$. This is the expected result for any signal exhibiting only one Hurst exponent. It is worth stressing again that Eq. (3) is inapplicable, except at very large values of ℓ (see Fig. 1).

Before proceeding, notice that a change in the sampling time Δt requires a reciprocal change in ℓ, for the results to be comparable within an interval of fixed length $t = \ell \, \Delta t$. Similarly, the signal differences $d_i(k)$ will have to be computed across a correspondingly changed value of k. Therefore, the relevant quantity to consider, in order to ensure invariance of the results under modification of the sampling time, is the ratio

$$\ell' = \ell/k \, . \tag{15}$$

This can also be understood by computing $E_i(\ell; k)$ through a sum including ℓ/k increments over disjoint subintervals only: the formula in Eq. (9), generally used to increase the statistics, can in fact be split into k terms, each representing a sum of ℓ/k addends with a shifted origin.

In the discussion of more general cases, we shall relax the condition that the increments $d_i(k)$ obey Gaussian statistics while still assuming their mutual independence in the first step of the deduction (obviously, exactly the converse is true for fBms with $H \neq \frac{1}{2}$). Correlations will be later accounted for, together with non-Gaussian statistics, by the introduction of two parameters. Because of its simplicity and independence of the details of the signal's statistics, this approach is general and powerful enough to reproduce scaling behaviour originating from quite different sources, such as turbulent flows, EEG recordings [14], and, of course, fBms.

A further simplification makes the argumentation particularly easy to follow. Namely, we split the interval $I_E = [0, E]$ into r equal subintervals of length $\Delta E = E/r$, where $r \gg 1$ is arbitrary: it will be allowed to diverge in order for ΔE to vanish asymptotically. Consequently, we assume that $E(\ell)$ can only increase in discrete steps of amplitude ΔE and write

$$E(\ell; k) = \Delta E(s_1 + s_2 + \cdots + s_{\ell'}) \, , \tag{16}$$

where ℓ' replaces ℓ/k for the above mentioned reason. The symbols s_i are chosen at random according to the probability of d_i^2 as

$$s_i = \begin{cases} 0 & \text{if } d_i^2 \leqslant \Delta R \, , \\ 1 & \text{otherwise} \, , \end{cases} \tag{17}$$

where ΔR is a suitable threshold value which depends on r and separates the distribution $P(d^2)$ into two parts.

In this way, the build-up of $E(\ell)$ is reduced to a one-directional random walk with a binary choice of step sizes, the probabilities of which will be denoted by p_0 (no displacement) and $p_1 = 1 - p_0$ (one step upwards). The walker's position is represented by the symbolic sequence $S_{\ell'} = s_1 s_2 \cdots s_{\ell'}$ and the stair to be climbed contains r steps. Then, the event $E(\ell; k) \in J_E(\Delta E) = (E, E + \Delta E)$ will occur if and only if the top of

the stair is reached at "time" $\ell' = \ell/k$. Hence, we need to estimate the probability that $S_{\ell'}$ contains r 1's and $m = \ell' - r$ 0's. Clearly, ℓ', r, and m are proportional to one another, and $\ell' \geqslant r$: in fact, ℓ' is the number of trials and r the number of successes. The desired density

$$\rho_\ell(E) = P(E(\ell; k) \in J_E(\Delta E))/\Delta E , \qquad (18)$$

is then obtained from Ref. [15]

$$P(E(\ell; k) \in J_E(\Delta E)) = \begin{pmatrix} \ell' - 1 \\ \ell' - r \end{pmatrix} p_0^{\ell' - r} p_1^r = \frac{\ell' - m}{m} B(m, \ell'; p_0) , \qquad (19)$$

where $B(m, \ell'; p_0)$ is the binomial distribution for m successes (the replacement of r with $\ell' - m$ made here actually exchanges the meaning of "success" and "failure" for r and m) with probability p_0 in ℓ' trials. This can be approximated by the Poisson distribution

$$P(m, \lambda) = \frac{\lambda^m}{m!} e^{-\lambda} , \qquad (20)$$

if $\ell' \to \infty$ and $p_0 \to 0$ at constant $\lambda = p_0 \ell'$. Furthermore, Eq. (17) shows that p_0 is the probability for d_i^2 to lie in $[0, \Delta R]$. In general, the density of d^2 and the correlations among the terms in the sum (9) may lead to a density $\rho_\ell(E)$ with (one or more) singularities, in analogy with a "fractal" measure. Therefore, we account for this possibility by introducing a dimension-like quantity D and postulating the "mass-radius" scaling relation

$$p_0 \sim a(\Delta R)^D = a\frac{E^D}{r} , \qquad (21)$$

where a is a proportionality constant. Notice that ΔR has only a formal meaning (as a radius) and the scaling in Eq. (21) actually represents a fraction r of the overall "mass" in a sphere of radius E. The purpose of D is to condensate information about the cumulative effect of correlations and non-Gaussian fluctuations over the whole interval $I_E = [0, E]$. As customary in the theory of turbulence, however, I_E is still considered small enough for $E(\ell; k)$ to be actually a local average. Analogously, D is to be interpreted as a local dimension, the fluctuations of which will be characterized by a generalized dimension D_p, defined through the moments of $\rho_\ell(E)$, in analogy with Renyi's generalized dimensions D_q [16].

Using Eq. (21), the parameter λ of the Poisson distribution (20) reads

$$\lambda(E) = (E/E_0)^D , \qquad (22)$$

where E_0 is a normalization constant, independent of ℓ. We further introduce a parameter μ as the ratio

$$\mu = \frac{m}{\ell'} = \frac{mk}{\ell} \qquad (23)$$

between the number of "successes" and trials, thus characterizing the degree of "intermittency" in the process: walks advancing by several small steps will accordingly be

distinguished from walks advancing by a few large steps, for the same values of E. Collecting all terms, one finally obtains

$$\rho_\ell(E) = \frac{D}{E_0} \frac{(E/E_0)^{mD-1}}{\Gamma(m)} e^{-(E/E_0)^D} , \tag{24}$$

where the dependence of m on ℓ and k is expressed through Eq. (23). This density was considered by Essenwanger [17] in a different context, as an extension of the Weibull distribution. Upon multiplication by $\varepsilon^p = (E/\ell)^p$ and integration, one obtains an analytical expression for the expected moments of order p which depends on the two parameters D and μ. Since these quantities are locally fluctuating, in analogy with local Hölder exponents of multiaffine curves or local dimensions and Lyapunov exponents in dynamical systems, their global counterparts in the scaling relation depends on the order p. Therefore, we indicate them with D_p and μ_p and write the refined scaling law as

$$\langle \varepsilon^p(\ell) \rangle \sim \left(\frac{\ell}{k} \right)^{-p} \frac{\Gamma(\mu_p(\ell/k) + p/D_p)}{\Gamma(\mu_p(\ell/k))} . \tag{25}$$

Notice that, while the presence of k in the first factor (power-law) is irrelevant for the ℓ-scaling, it is essential in the second (gamma functions), since the arguments have to be adimensional and, therefore, can only contain ratios of times. Since this scaling formula is valid at fixed k and variable ℓ, the former parameter has been omitted in the argument of ε on the l.h.s. (a complete formula will be proposed in the following section).

The continuous curves in Fig. 1 represent fits obtained from Eq. (25) with $p = 2$, different values of μ_2, and the fixed value $D_2 = 1$. Indeed, for $k = 1$ and $\mu_p = 1/2$, Brownian motion scaling (Eq. (14)), is recovered with $D_p = 1$, $\forall p$. Fig. 2 illustrates how moments $\langle \varepsilon^p(\ell) \rangle$, computed at $p = -1$ (a), 0.5 (b), and 4 (c), are well reproduced by Eq. (25) for data of different origin: (squares) refer to Brownian motion, (triangles) to wind velocity data sampled at 3 kHz in an atmospheric flow with Taylor–Reynolds number 10 000, and circles to a non-REM stage 4 in a sleep EEG recording (128 Hz). The estimated values of D_p and μ_p for the nine plots are reported in Table 1. In these calculations, k was 5: hence, μ_p differs from $\frac{1}{2}$ for the Brownian motion ($H = \frac{1}{2}$) example, since the sum in Eq. (9) involves correlations among the addends, arising from $k - 1$ overlapping indices.

4. Discussion and extensions of the refined scaling law

In our model, the distribution of $d_i(k)$ has been split into two contributions, separated by the threshold value ΔR (Eq. (17)). In turn, ΔR has been characterized by the two parameters D and μ, as it can be seen by writing

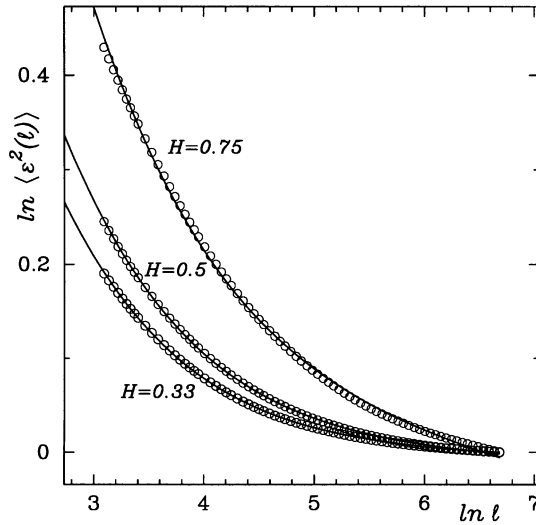$$\left(\frac{E}{\Delta R} \right)^D = r = \ell'(1 - \mu) . \tag{26}$$

Fig. 1. Plot of $\langle \varepsilon^2(\ell) \rangle$ vs. ℓ for three fractional Brownian motions with Hurst indices $H = 0.33$, 0.5, and 0.75, in a doubly-logarithmic scale. The continuous curves represent fits obtained from Eq. (25).
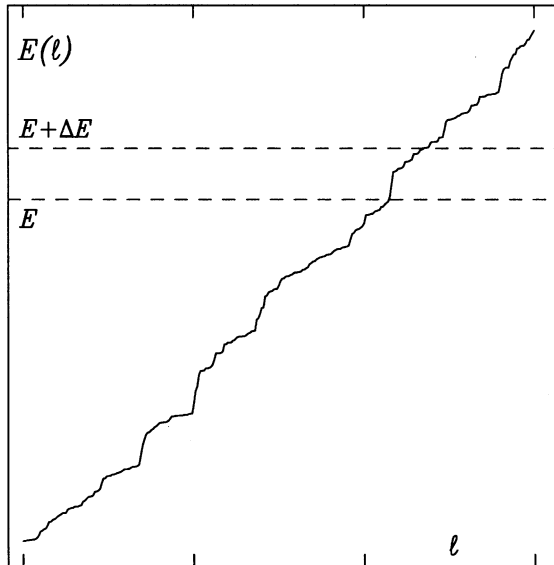

Fig. 2. Plot of $E(\ell; k)$ vs. ℓ for a fBm with $H = 0.33$ and $k = 5$.

Therefore, ΔR contains the relationship between the target value E of the sum (9) and the length ℓ' of the walker's path.

The connection of the refined law (25) with the power-law assumption Eq. (3) is readily established by noticing that the asymptotic behaviour of Eq. (25), for

Table 1
Values of the parameters τ_p and μ_p for the fits presented in Fig. 3

System	p	D_p	τ_p	μ_p
Brownian motion	-1	0.993	-0.007	0.95
	0.5	0.999	0.0006	0.87
	4	1.002	-0.008	0.75
Atmospheric turbulence	-1	0.84	-0.19	1.1
	0.5	0.956	0.023	0.86
	4	1.06	-0.23	0.08
Non-REM 4 sleep stage	-1	0.935	-0.07	0.87
	0.5	0.98	0.01	0.78
	4	1.216	-0.71	1.30

$(\mu\ell)/k \gg p/D_p$, is

$$\langle \varepsilon^p(\ell) \rangle \sim \ell^{-p+p/D_p} . \tag{27}$$

Therefore, by setting

$$D_p = \frac{p}{p + \tau_p} , \tag{28}$$

we relate the new parameter D_p with the exponent τ_p of the conventional power-law scaling (3), in the limit $\ell \to \infty$ (estimated values of τ_p are also reported in Table 1). Hence, $D_p = 1$ is equivalent to $\tau_p = 0$: this is the case of mono-affine signals, as illustrated in Fig. 1. Actually, this occurs for all signals with stationary increments, even if multi-affine, for ℓ sufficiently large, since $\varepsilon(\ell)$ must then converge to a finite value. Weak forms of nonstationarity may reflect in fluctuations around a finite value. Therefore, evaluating τ_p is meaningful only before this final regime sets in. The importance of Eq. (25) lies in its ability to reproduce the moments very accurately even for small ℓ with the correct value of τ_p. In fact, the asymptotic form (27), which would enable one to apply Eq. (3), may start to hold, depending on μ and k, for such large values of ℓ that the moment $\langle \varepsilon^p \rangle$ already "rests" in the above-mentioned plateau. Since there $\tau_p = 0$, power-law scaling would come too late to detect anything interesting.

The generalized dimension D_p, as already commented upon, describes the clustering of the values $E(\ell)$, for all values of ℓ, as caused by the sequence of increments $d_i(k)$ (vertical axis in Fig. 3): hence, $D_p \neq 1$ means that the "points" $E(1)$, $E(2)$, ..., $E(\ell)$ constitute a finite sample of a measure $\sigma(E)$ with singular behaviour. Fig. 4 shows such a distribution (curve a, log–linear scale) computed from wind velocity data measured in the atmosphere at 3 kHz. The values of ℓ were in the range [6,600] and $k = 5$. Notwithstanding the finiteness of both statistics and resolution, the plot exhibits a sizeable accumulation around $E = 0$. The curves depend on k: similar results, however, are obtained for signals from quite different sources. On the contrary, a fractional Brownian motion with Hurst index $H = 0.33$ shows no singularity at all (Fig. 4, curve b).
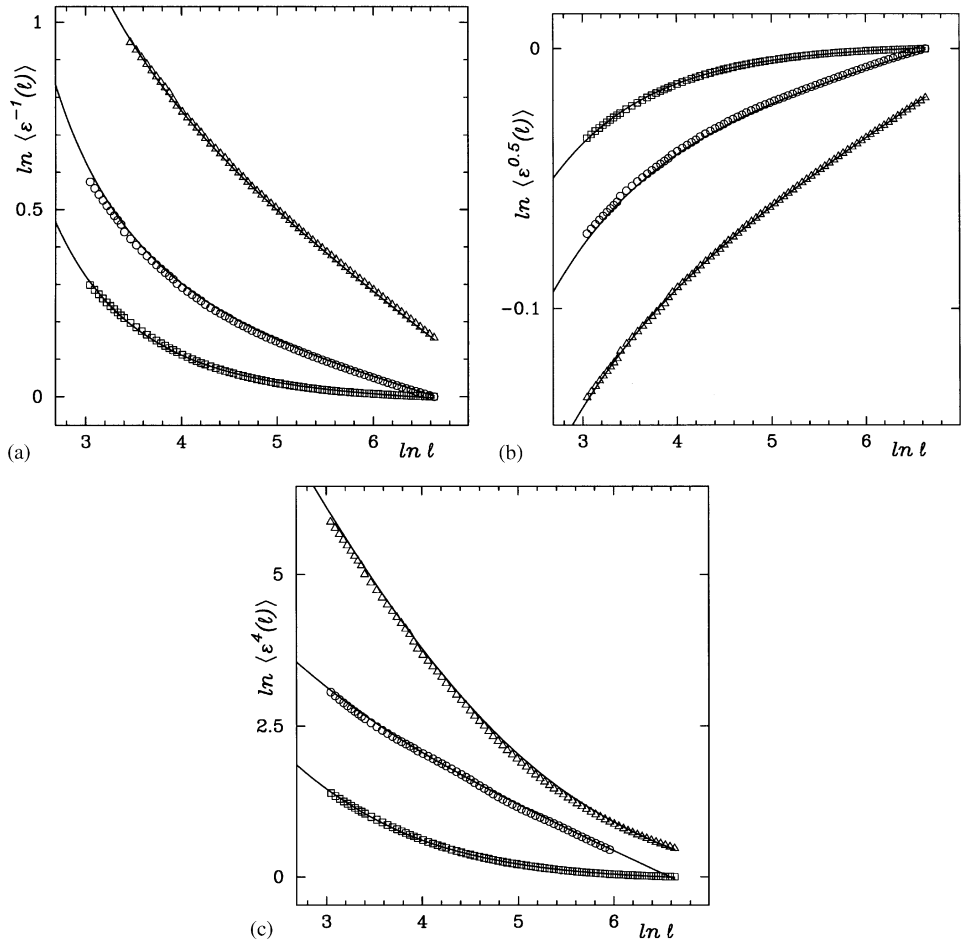
Fig. 3. Moments $\langle \varepsilon^p(\ell) \rangle$ vs. ℓ (in a log–log scale), computed at $p = -1$ (a), 0.5 (b), and 4 (c), on data from Brownian motion (squares), a non-REM stage 4 in a sleep EEG recording (circles), and atmospheric turbulence with Taylor–Reynolds number 10 000 (triangles). The results of fits provided by Eq. (25) are drawn using solid lines. The curves have been vertically displaced for clarity.

Notice that $\sigma(E)$ is computed using all values of ℓ in some interval, whereas $\rho_\ell(E)$ is the density for the variable $E(\ell; k)$ at fixed ℓ. Hence,

$$\sigma(E) = \sum_{\ell = \ell_1}^{\ell_2} \rho_\ell(E) \sim \left(\frac{E}{E_0} \right)^{D-1} , \qquad (29)$$

where the asymptotic power-law behaviour is valid for $\ell_1 \to 0$ and $\ell_2 \to \infty$. Indeed, curve "a" in Fig. 4 exhibits power-law scaling in some range. The singularity is smoothened off at smaller E, because of the resolution constraint imposed by the choice $k = 5$ (necessary for this kind of turbulent data to avoid measurement noise).
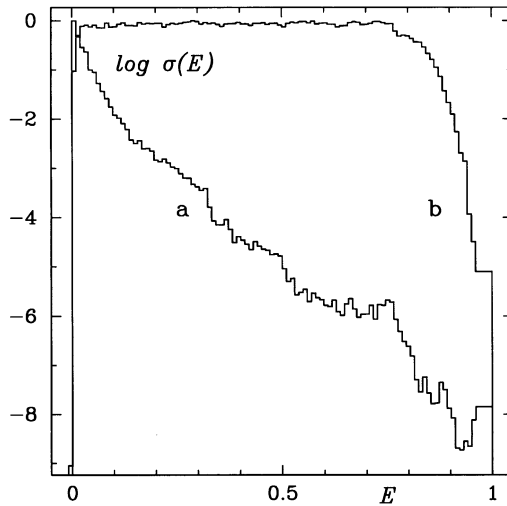
Fig. 4. Logarithm of the density $\sigma(E)$ of the (generalized) variation $E(\ell; k)$ computed for all values of $\ell \in [6, 600]$ from wind velocity data (a), sampled at 3 kHz ($k = 5$). Analogous curve for an fBm (b) with $H = 0.33$, $k = 5$. The variable E has been normalized in $[0, 1]$ and the plots have been vertically shifted for clarity.

At larger E, a steeper falloff occurs.[4] This is due both to lack of statistics and to the inadequacy of a single "dimension" value D for the characterization of the whole distribution in multi-affine systems, such as turbulent ones. The moments, however, are well reproduced by Eq. (25) when fitted using a p-dependent D_p. Whenever $D_p = 1$, no singularity exists and $\rho_\ell(E)$ is essentially a Poisson distribution. This is confirmed for Brownian motion (fractional or not). In general, however, this is not true and the Essenwanger distribution (24) provides a good model.

The refined scaling law (25) solves a number of outstanding problems which generally make the conventional power-law approach (3) unsuitable. Firstly, the evident bending of the curves (in log–log plots) is now well reproduced. This yields estimates of τ_p consistent throughout a much wider range than before: for the mono-affine signals used to produce Fig. 1, the ℓ-range is infinite. Secondly, a near-invariance of τ_p with k (in a suitable range) is achieved, a feature which has never been addressed before, since it was implied by the (wrong) power-law assumption (3). Finally, the convergence of $\langle \varepsilon^p(\ell) \rangle$ to a constant (up to eventual fluctuations) for very large ℓ is made evident by the form of the new scaling law, especially in the case $\tau_p = 0$ (Fig. 1) which would be badly approximated by Eq. (3).

The second parameter, μ_p, is actually new in the present theory. As already mentioned in the previous section, it represents the fraction of addends $d_i^2(k)$ which are smaller than ΔR in the sum (9). Eq. (26) links μ and D to ΔR locally. Small

---

[4] These considerations refer to log–log plots, whereas a log–linear one has been shown in Fig. 4, in order to distinguish the two curves more clearly in the whole range.

values of μ_p correspond to strong bending of the log–log curves of $\langle \varepsilon^p \rangle$ versus ℓ, i.e., to substantial deviations from the power-law conjecture (3). It is apparent from Fig. 1 that μ_p depends on the Hurst exponent H for fractional Brownian motions (which cannot be distinguished from one another on the basis of τ_p, since $\tau_p = 0$ for all of them). The dependence of μ_p on H, however, is not straightforward since it implies correlations among the terms in the sum (9) and the value of k. Therefore, this issue will be addressed in a separate publication.

Before presenting two extensions of the refined scaling law, it is worth commenting on its relationship with a formula which has been proposed in Ref. [18] in the context of dimension estimators for sets of data points. Consider a set $A = \{x_i\}$ of n points in an E-dimensional Euclidean space and compute the distance $\delta_i(m)$ between the ith point and its mth nearest-neighbour. In early work in the field of dynamical systems [19,20], it was conjectured that the moments

$$\langle \delta^\gamma(m) \rangle \sim m^{\gamma/\tilde{D}(\gamma)} . \tag{30}$$

scaled like powers of m for fixed n and that the exponent was related to the actual dimension $\tilde{D}(\gamma)$ of the set A: notice that this $\tilde{D}(\gamma)$ is a different function than Renyi's generalized dimension D_q. Actually, as shown in Ref. [18] and further illustrated in physical journals [21–23], the averages are better reproduced by the formula

$$\langle \delta^\gamma(m) \rangle \sim \frac{\Gamma(m + \gamma/\tilde{D}(\gamma))}{\Gamma(m)} n^{-\gamma/\tilde{D}(\gamma)} , \tag{31}$$

especially for $n \gg m \gg m/n$. Incidentally, the scaling with the number of points n is indeed a power law and was proposed in Refs. [24,25].

In the deduction of Eq. (31), it is assumed that the m points in a hyperball B_δ of size $\delta_i(m)$ are uniformly and identically distributed and that observing the samples that fall within B_δ is equivalent to performing a sequence of Bernoulli trials. In our approach, the "points" are the successive values $E(1), E(2), \ldots, E(\ell)$, and the ball's radius is E: evidently, these "points" are not identically distributed. Moreover, the distribution within the "ball" of size E is not assumed to be constant but is characterized by the parameters D and μ. It must be noted that the latter is a new ingredient which does not result at all from the procedure of Ref. [18].

Finally, the expected power-law scaling of the averages with k (see Eq. (12) for a special case) is quantitatively reproduced by the refined formula (25): in fact, its behaviour for fixed ℓ and variable k is extremely close to k^z, for some z. Therefore, the complete scaling law, in terms of ℓ and k, can be written as

$$\langle \varepsilon^p(\ell; k) \rangle \sim \frac{k^{Z_p}}{C + k^{-z_p}} \left(\frac{\ell}{k} \right)^{-p} \frac{\Gamma(\mu_p(\ell/k) + p/D_p)}{\Gamma(\mu_p(\ell/k))} , \tag{32}$$

where Z_p and z_p are suitable exponents and C a constant, all to be determined from a fit (at fixed ℓ). Indeed, $C = 0$ and $Z_p + z_p = pH$ for fractional Brownian motion with Hurst index H. Numerically, $C = 0$ also for more general, mono-affine signals. Turbulent and EEG signals, however, are characterized by nonzero values of C: typical values are of the order of 0.1 for $p = 2$. For large k, the ratio of the Gamma functions in Eq. (32)
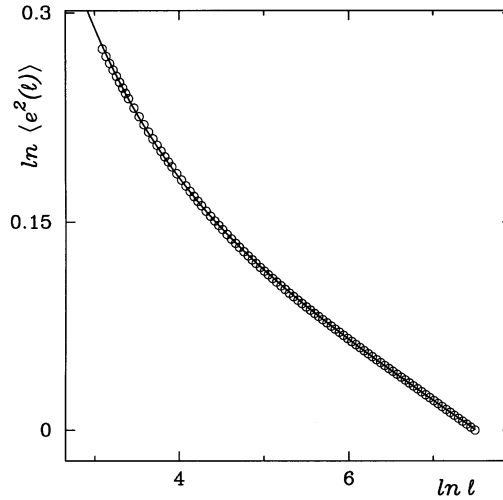
Fig. 5. Plot of $\langle e^2(\ell) \rangle$ vs. ℓ for atmospheric turbulent data in a doubly-logarithmic scale. The quantity e, analogous to ε and defined in Eq. (33), has been computed using $k = 8$. The continuous curve represents a fit obtained from Eq. (25).

scales like k^{-p/D_p}: hence, $Z_p + z_p \approx p/D_p + \zeta_p$, for $C = 0$, and $Z_p \approx p/D_p + \zeta_p$, for $C \neq 0$; the exponent ζ_p having been defined in Eq. (1).

As a last remark, we show that the improved formula applies to quite general sums of nonnegative arguments, such as the average variation

$$e_i(\ell;k) = \frac{1}{\ell} \sum_{j=i}^{i+\ell-1} |d_j(k)| , \tag{33}$$

of the signal over an interval of length ℓ, which is analogous to $\varepsilon_i(\ell;k)$: the difference being the replacement of the square increments with their absolute value. A plot of $\langle e^2(\ell;k) \rangle$ versus ℓ, obtained from atmospheric turbulent data using $k = 8$, is reported in Fig. 5. The fit yielded $\tau_2 = -0.04$ (we use the same symbol as for ε, for simplicity) and $\mu_2 = 3.28$: the fit curve clearly is in perfect agreement with the experiment in the whole range.

The quantity in Eq. (33) has been employed, for example, in the analysis of financial data, compared with fBms [26], albeit with $k = \ell$. As our analysis shows, exponent estimates based on the commonplace power-law assumption cannot account for the bending of the curves in a log–log plot and may lead to wrong results, such as $\tau_p \neq 0$ for fractional Brownian motion. Indeed, the fits with the refined formula yield $\tau_p = 0$ for mono-affine signals also using the observable $e(\ell;k)$ of Eq. (33) above. There cannot be any bell-shaped τ_p curve for such processes. Differences can be quantified by the new parameter μ_p, which we have introduced in our approach.

5. Conclusions

We have presented evidence that the moments of the (generalized) variation of multi-affine signals, either numerically generated or recorded in physical experiments, do not exhibit power-law scaling but deviate considerably from it, especially when the order $|p|$ is much larger than 1. A stochastic model has been introduced to reproduce the behaviour. This not only allowed us to obtain very accurate estimates of the scaling exponent τ_p, which is carried over from the conventional scaling approach, but also provided a second parameter which can be profitably employed to distinguish the various signals. Furthermore, the exponent τ_p has been related to a dimension-like quantity, D_p, which opens new possibilities of interpretation for the analysis of turbulence data.

Acknowledgements

References

[1] J.-P. Bouchaud, A. Georges, Phys. Rep. 195 (1990) 12.
[2] M.F. Shlesinger, G.M. Zaslavsky, U. Frisch (Eds.), Lévy Flights and Related Topics in Physics, Springer, New York, 1995.
[3] B.B. Mandelbrot, The Fractal Geometry of Nature, Freeman, San Francisco, CA, 1982.
[4] B.B. Mandelbrot, Multifractals and $1/f$ noise: wild self-affinity in physics (1963–1976), Selected works of Benoit B. Mandelbrot, Vol. N, Springer, New York, 1999.
[5] A.S. Monin, A.M. Yaglom, Statistical Fluid Mechanics, Vols. 1 and 2, MIT Press, Cambridge, MA, 1971,1975.
[6] A.N. Kolmogorov, J. Fluid. Mech. 13 (1962) 82.
[7] A.M. Obukhov, J. Fluid. Mech. 13 (1962) 77.
[8] A.N. Kolmogorov, Dokl. Akad. Nauk SSSR 30 (1941) 301.
[9] R. Badii, P. Talkner, unpublished.
[10] B.B. Mandelbrot, J.W. Van Ness, SIAM Rev. 10 (1968) 422.
[11] R. Badii, P. Talkner, Phys. Rev. E 59 (1999) 6715.
[12] G. Chan, A.T.A. Wood, in: R. Payne, P. Green (Eds.), COMPSTAT, Physica-Verlag, Heidelberg, 1998, p. 233.
[13] A. Papoulis, Probability, Random Variables, and Stochastic Processes, 2nd Edition, McGraw-Hill, Singapore, 1984.
[14] R. Badii, Y. Shen, P.F. Meier, unpublished.
[15] W. Feller, An Introduction to Probability Theory and its Applications, 3rd Edition, Vol. 1, Wiley, New York, 1968.
[16] A. Renyi, Probability Theory, North-Holland, Amsterdam, 1970.
[17] O.M. Essenwanger, Applied Statistics in Atmospheric Science, A. Frequency Distribution and Curve Fitting, Elsevier, Amsterdam, 1976.
[18] K.W. Pettis, T.A. Bailey, A.K. Jain, R.C. Dubes, IEEE Trans. Pattern Anal. Machine Intell. PAMI-1 (1979) 25.
[19] Y. Termonia, Z. Alexandrowicz, Phys. Rev. Lett. 51 (1983) 1265.
[20] J. Guckenheimer, G. Buzyna, Phys. Rev. Lett. 51 (1983) 1438.

[21] R.L. Somorjai, in: G. Mayer-Kress (Ed.), Dimensions and Entropies in Chaotic Systems, Springer, Berlin, 1989, p. 137.
[22] P. Grassberger, Phys. Lett. A 107 (1985) 101.
[23] P. Grassberger, Phys. Lett. A 128 (1988) 369.
[24] R. Badii, A. Politi, Phys. Rev. Lett. 52 (1984) 1661.
[25] R. Badii, A. Politi, J. Stat. Phys. 40 (1985) 725.
[26] K. Ivanova, M. Ausloos, Eur. Phys. J. B 8 (1999) 665.